

# UWB Low-Profile Tightly Coupled Dipole Array With Integrated Balun and Edge Terminations

Ioannis Tzanidis, *Member, IEEE*, Kubilay Sertel, *Senior Member, IEEE*, and John L. Volakis, *Fellow, IEEE*

**Abstract**—Tightly coupled phased arrays (TCPAs) provide UWB performance due to their strong inter-element coupling. However, in finite tightly coupled phased array realizations, mutual coupling is reduced near the array edges, causing the edge elements to become narrowband. To address this issue, a nonuniform array excitation scheme, referred to as “characteristic mode (CM) excitation,” was recently proposed. A more practical alternative for designing UWB tightly coupled phased arrays is proposed here. In this paper, we present a strategy that employs uniform excitation of the central array elements and short-circuits the periphery elements. We report that at least for medium size arrays, this approach provides up to 3 dB more gain and 50% higher efficiency than typical resistive termination. This concept is demonstrated using a  $7 \times 7$  linearly polarized dipole array,  $60.96 \text{ cm} \times 60.96 \text{ cm}$  ( $2' \times 2'$ ) in size, for operation from 200 MHz–600 MHz. Feeding of the active elements is challenging due to several constraints on the feed design, including balanced to unbalanced transitions, impedance transformations, common mode suppression, compact size, low cost, etc. To address these issues we propose a novel array feed using a compact, ultrawideband balun (with 10:1 bandwidth for  $\text{VSWR} < 2$ ). Simulated and measured data are provided for broadside and  $30^\circ$  scan in the H-plane.

**Index Terms**—Dipole arrays, finite array terminations, tightly coupled phased arrays (TCPAs), ultrawideband arrays, wideband balun, wideband impedance transformer.

## I. INTRODUCTION

THERE is continuing interest to design UWB apertures that are concurrently small in size and highly conformal. Such apertures find use in the military sector (imaging sensors) and in commercial applications (4G telecommunication standards, such as LTE). Towards this goal, the newly introduced phased arrays known as *tightly coupled phased arrays* (TCPAs), exhibit UWB performance (5:1 bandwidth) and are of low profile (as thin as  $\lambda/10$ , where  $\lambda$  is the wavelength at the lowest operational frequency) [1]. The wide bandwidth of tightly coupled phased arrays is attributed to the strong mutual coupling between their elements, effectively emulating a sheet of uniform current. Most notably, this capacitive coupling serves to cancel the inductance contributed by the array ground plane. As such,

Manuscript received January 02, 2012; revised August 28, 2012; accepted February 09, 2013. Date of publication March 07, 2013; date of current version May 29, 2013. This work was supported by the Air Force Research Laboratories and Lockheed Martin Corp (10010042) under the PO KRRTP355AE.

The authors are with ElectroScience Lab., The Ohio State University, Columbus, OH 43212 USA (e-mail: tzanidis.1@osu.edu; sertel.1@osu.edu; volakis.1@osu.edu).

Color versions of one or more of the figures in this paper are available online at <http://ieeexplore.ieee.org>.

Digital Object Identifier 10.1109/TAP.2013.2250232

large bandwidths on the order of 5:1 can be achieved [1]. Research in tightly coupled arrays has been very intense in the past 10 years [1]–[15]. However, when realizing a practical array, issues such as feeding and array terminations become critical to performance and have not been systematically addressed. This paper presents our findings on these practical aspects of finite size tightly coupled phased arrays.

In finite size arrays, mutual coupling diminishes near the array edges. Thus, the array periphery elements become narrowband. Further, periphery elements are prone to severe impedance mismatch and exciting them degrades the array bandwidth. To address this issue, we introduced in [6] a tapered excitation that follows the characteristic modes of the array structure. Alternatively, the finite array edge effects can be mitigated by terminating the periphery elements with matched resistors. This improves the array bandwidth, but can lead to low efficiency [16]. Here, we demonstrate that short-circuit terminations of the periphery elements provides for good tradeoff between impedance bandwidth and realized gain. It also leads to more consistent radiation patterns over the operational bandwidth.

Nevertheless, a major challenge in realizing a tightly coupled phased array is the design of the array feed. Specifically, to realize the array bandwidth it is necessary to design a feed balun that operates over the entire bandwidth. The balanced feed must also provide for a  $50 \Omega$  (coaxial line) to  $200 \Omega$  (typical for dipole arrays) transition. Also, for convenient integration, the balun need be compact in size, low cost, and capable of low insertion loss over a large bandwidth. A further issue to be addressed relates to the possible common mode supported by the feed structure. These common modes are related to the length of the path formed by the feed lines and the element geometry [17]. Thus, with proper design, they can be pushed out of the operational range [5].

Various array feeds have been proposed [2], [4], [5], [18]. Section III, presents a novel, printed array feed balun with integrated impedance transformer ( $50 \Omega$ – $200 \Omega$ ) that is much more broadband (10:1) and simple than those considered previously. The proposed feed is comprised of two short printed sections: a coplanar waveguide (CPW) and a coplanar strips (CPS) section, interconnected with a compact, ultrawideband coiled balun. Simulated and measured data are presented for broadside and a  $30^\circ$  scan in the H-plane.

## II. EDGE ELEMENT TERMINATIONS FOR IMPROVING BANDWIDTH

The specific array under consideration, depicted in Fig. 1, has a size of  $60.96 \text{ cm} \times 60.96 \text{ cm}$  ( $2' \times 2'$ ) and a thickness of  $15.24 \text{ cm}$  ( $6''$ ). Accordingly, the array unit cell was chosen to

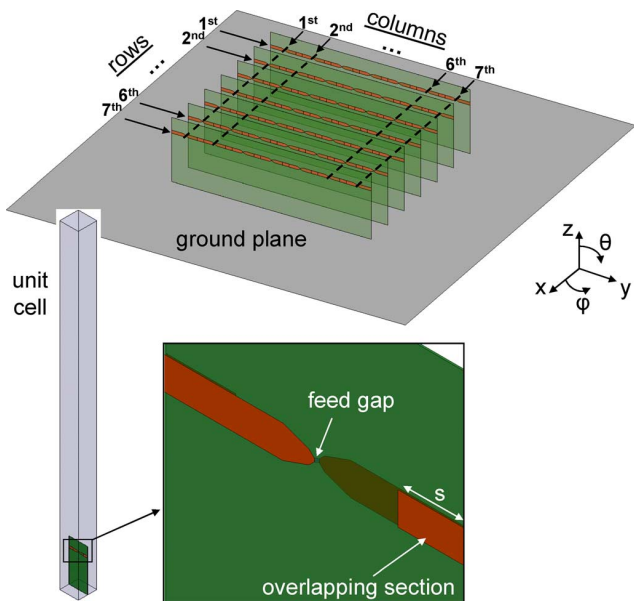


Fig. 1. Illustration of the  $7 \times 7$  linearly polarized overlapping dipole array. Array size is  $60.96 \text{ cm} \times 60.96 \text{ cm}$  ( $2' \times 2'$ ), thickness  $15.24 \text{ cm}$  ( $6''$ ) and the ground plane size is  $121.92 \text{ cm} \times 121.92 \text{ cm}$  ( $4' \times 4'$ ). The infinite array unit cell is also shown. It is depicted enclosed within a rectangular box, defining the periodic cell in the modeling computer code.

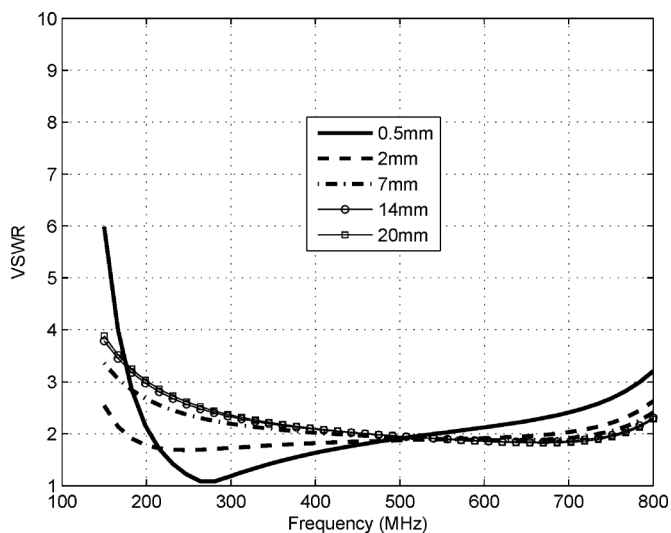


Fig. 2. VSWR versus frequency for an infinite dipole array with overlapping elements as in Fig. 1. Several curves are shown corresponding to different values of the overlapping dipole section  $s$ . System impedance was  $Z_0 = 200 \Omega$ .

be  $8.71 \text{ cm} \times 8.71 \text{ cm}$  ( $2'/7 \times 2'/7$ ) for a  $7 \times 7$  element array. As shown in [1]–[3], the impedance bandwidth of the infinite array (for  $\text{VSWR} < 2$ , referenced to  $Z_0 = 200 \Omega$ ) can be maximized by tuning the mutual capacitance between adjacent elements. In our case, this was done by adjusting the length,  $s$ , of the overlapping dipole section, as depicted in Fig. 1. It was found that within the range  $0.5 \text{ mm}$ – $20 \text{ mm}$ , for  $s = 2 \text{ mm}$  the achieved bandwidth can be maximized to cover from  $170 \text{ MHz}$ – $700 \text{ MHz}$  (see Fig. 2).

However, as already noted, this bandwidth is reduced when a finite array is considered. This is due to detuning of the peripheral array elements. To compensate for that, one can increase the overlapping section of the dipoles up to  $s = 20 \text{ mm}$  but only minor bandwidth improvements are achieved. Fig. 3

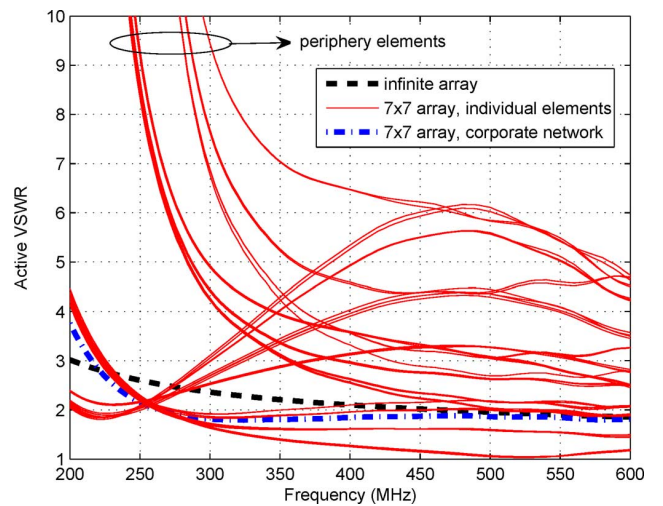


Fig. 3. Active VSWR of all elements in the  $7 \times 7$  array shown in Fig. 1. The dipole overlapping section,  $s$ , was increased to  $20 \text{ mm}$  to account for the weaker mutual coupling of the periphery elements. Each solid line curve in the plot corresponds to one of the array's 49 elements. The VSWR of the infinite array and that of a corporate feed are also shown. System impedance was  $200 \Omega$ .

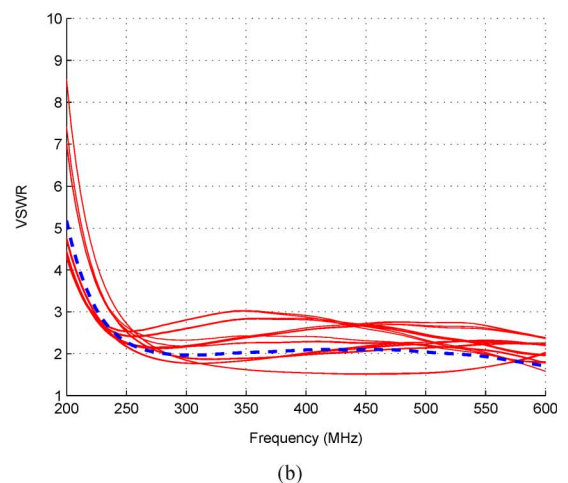
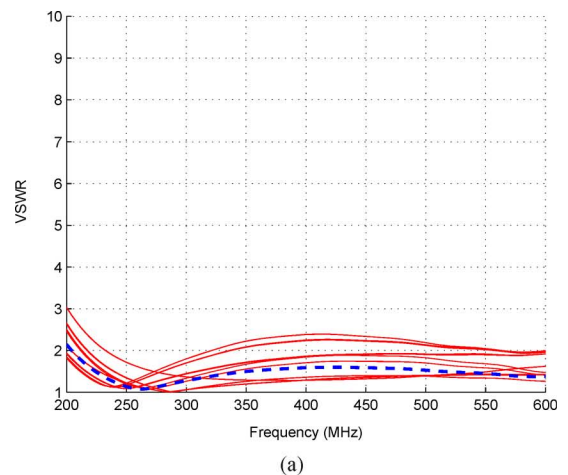


Fig. 4. Active VSWR of  $3 \times 7 = 21$  active elements of  $7 \times 7$  array shown in Fig. 1. 28 edge elements on first, second, sixth, and seventh columns of the array (see Fig. 1) are terminated in (a)  $200 \Omega$  resistors and (b) short-circuit.

shows the active VSWR of all 49 elements (49 curves plus 2 more for reference). It is clear that the  $\text{VSWR}_s$  vary significantly among the elements. In particular, the elements towards the array periphery are significantly detuned as compared to the

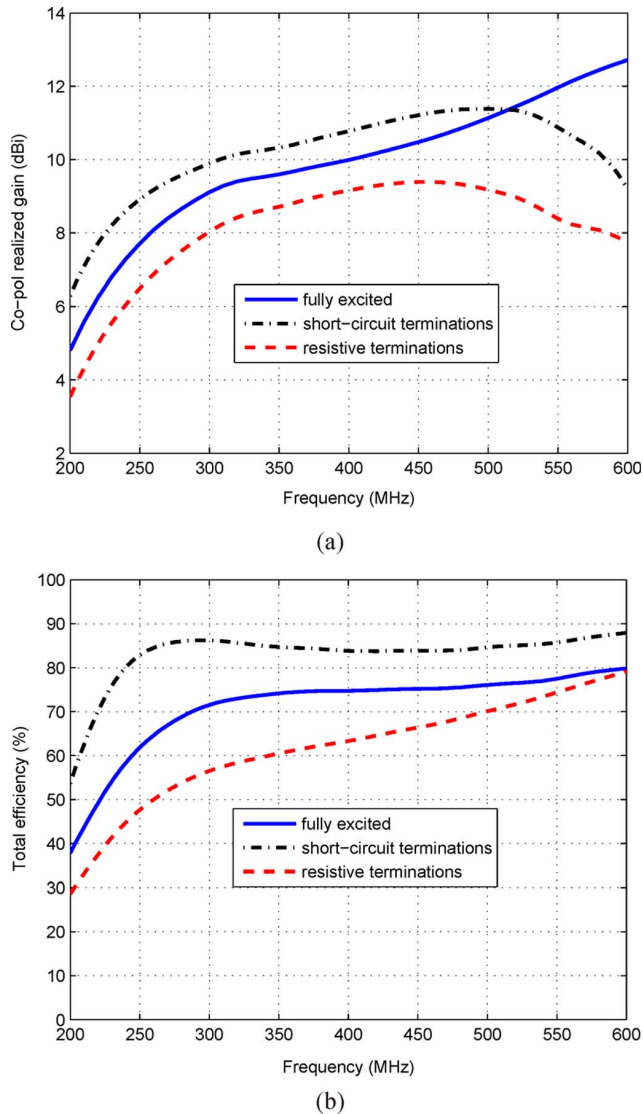


Fig. 5. (a) Co-pol. realized gain and (b) efficiency of the  $7 \times 7$  array shown in Fig. 1 under different excitations. Three cases are compared: uniformly excited array with no terminations and with its first, second, sixth, and seventh columns terminated in  $200 \Omega$  resistors and short-circuits.

infinite array VSWR. Therefore, the  $7 \times 7$  array's bandwidth is significantly smaller than its infinite counterpart. We note that the corporate feed VSWR appears quite good even though the individual elements are mismatched. This is because of the destructive interference of the reflected waves inside the power combiners. That is, the corporate feed obscures the individual array mismatches. This feed is not, therefore, a good choice for evaluating the array. Below, we discuss how to recover the lost bandwidth.

To mitigate finite array edge effects and improve bandwidth, various edge element termination techniques (resistive, short- and open-circuit) were investigated in [16]. It was found that among these loadings, the resistive termination provided for the lowest active VSWR. This was expected [see Fig. 4(a)], but the resistors resulted in losses and low efficiency. Therefore, it was concluded that short-circuit terminations of the peripheral array elements provided for a better tradeoff between impedance bandwidth and efficiency. The active VSWR<sub>s</sub> for the short-cir-

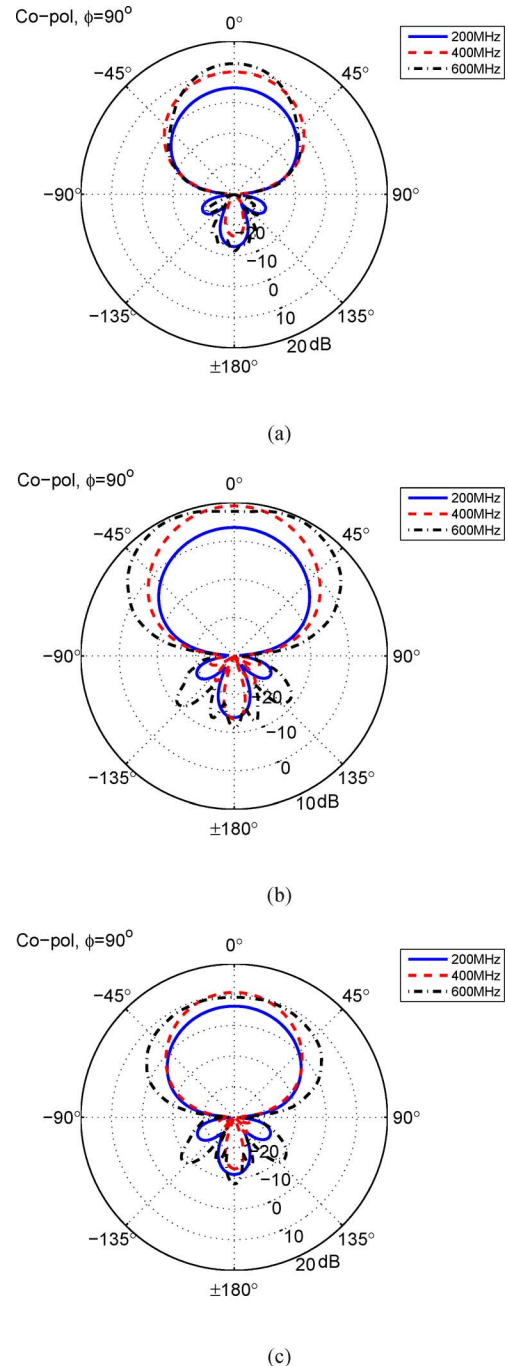


Fig. 6. Realized E-plane gain patterns for the  $7 \times 7$  array in Fig. 1 at 200 MHz, 400 MHz, and 600 MHz. Three excitation cases are compared: uniformly excited array with (a) no terminations, and with columns 1, 2, 6, 7 terminated in (b)  $200 \Omega$  resistors and (c) short-circuits. Please note the slightly different scale used in (b).

cuit terminations are given in Fig. 4(b). Also, Fig. 5 gives a comparison of the co-pol. realized gain and efficiency of the array in Fig. 1. The following three cases are compared: 1) uniformly excited array with no terminations, 2) with the first, second, sixth, and seventh columns terminated in  $200 \Omega$  resistors (see Figs. 1 and 3) with the same columns terminated in short-circuits. All reference impedances for the active VSWR calculations were  $Z_0 = 200 \Omega$ .

As seen, the short-circuit terminations provide inferior impedance bandwidth than resistive terminations, but the

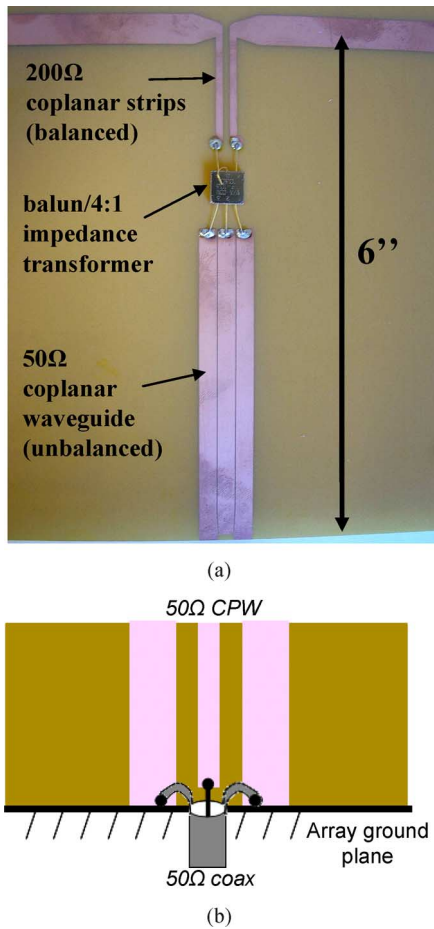


Fig. 7. Illustration of the balun/transformer used for feeding the array. (a) Unbalanced 50-Ω CPW interconnected to a balanced 200-Ω CPS via a lumped balun/impedance transformer. (b) Illustration of a CPW fed by a coaxial line.

shorted terminations provide 47% higher efficiency and lead to 2.75 dB higher realized gain. Specifically, the short-circuit terminations lead to greater than 80% efficiency over the whole band. In contrast, the resistive terminations have less than 70% efficiency. We also note that the cross-polarized gain remained below  $-34$  dBi, independent of termination type and across the whole band.

A shortcoming associated with periphery element terminations is a possible E-plane pattern split at higher frequencies. Particularly, in the case of resistive terminations, we observed a split of the main beam at 600 MHz in the E-plane, depicted in Fig. 6(b). It is clear that at 600 MHz the array pattern splits causing a  $\sim 2$  dB drop in the broadside gain. We do note, however, that for the short-circuited terminations the pattern split is mitigated, causing only 0.5-dB drop in gain. This can be seen in Fig. 6(c). For reference, the patterns of the fully excited array are also shown in Fig. 6(a). We remark, that the H-plane patterns were as expected and are omitted.

### III. FEED NETWORK AND MEASUREMENTS

As mentioned above, the feed of a tightly coupled phased array must realize two functions: 1) balanced to unbalanced transition (balun), and 2) impedance transformation with ratio

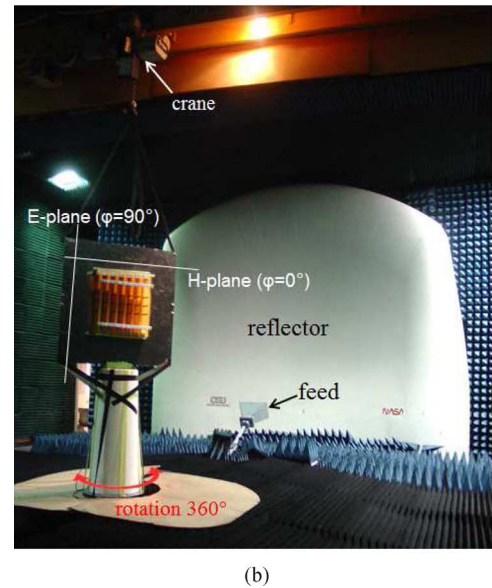
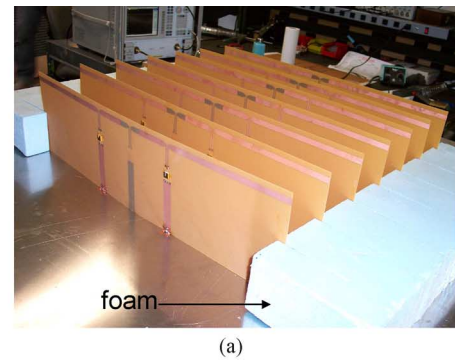


Fig. 8. (a) Illustration of the  $7 \times 7$  linearly polarized dipole array with integrated balun/impedance transformer and short-circuit terminations. For measurements  $3 \times 7 = 21$  elements were active and 28 elements were terminated. (b) Measurement setup in the compact range of ElectroScience Laboratory, Ohio State University.

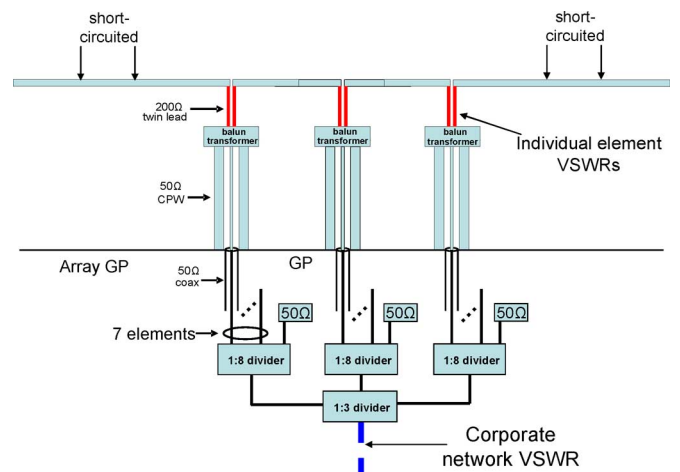


Fig. 9. Schematic of the array feed network (only one row of the array is shown).

4:1. Realizing these functions in the limited space under the array ( $\lambda/10$  at 200 MHz) is quite challenging. In particular, typical transmission line transformer baluns require at least  $\lambda/4$  length or height, and are not wideband. We found that among

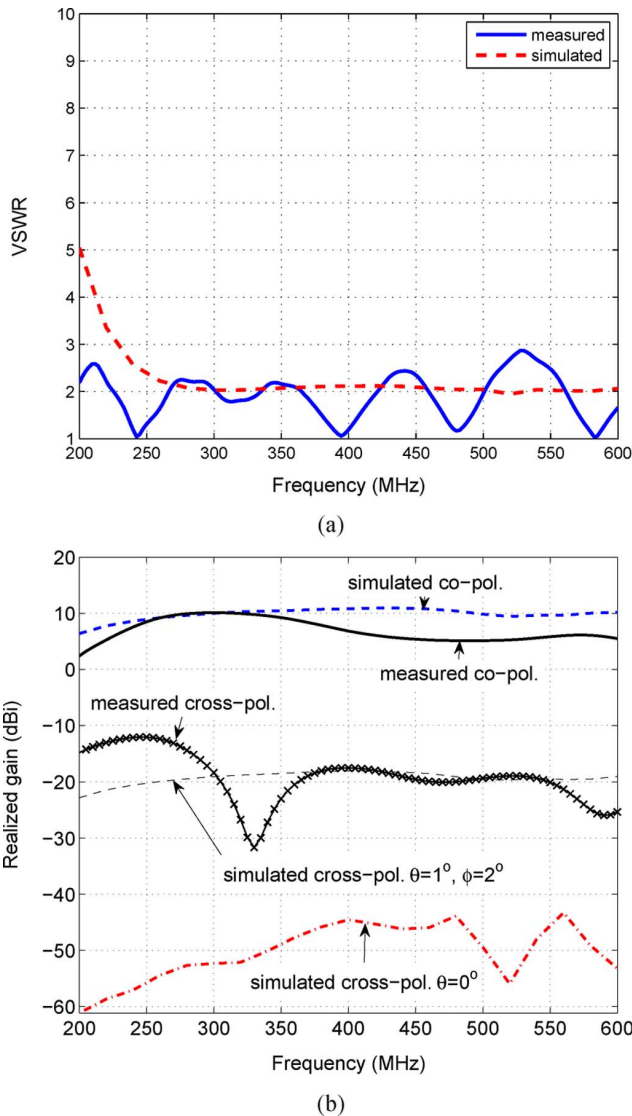


Fig. 10. Measured and simulated (a) VSWR and (b) realized gain for the array shown in Fig. 8(a) when radiating at broadside.

several existing baluns [19]–[25] none could be scaled or modified to fit our application. At this point for convenience, we used a commercially available, compact, coil-based ultrawideband balun/impedance transformer shown in Fig. 7(a) (part TP-103, MA-COM). As seen, the transformer is used to interconnect the 50- $\Omega$  coplanar waveguide (CPW) section with the 200- $\Omega$  coplanar strips (CPS) section. The CPW ground was soldered to the array ground plane and its center conductor was connected to a 50- $\Omega$  coax, through a hole on the ground plane [see Fig. 7(b)].

Also, we found that for the short-circuited (inactive) edge elements, the overlapping section had little effect on the performance. Therefore, we simplified their geometry by simply connecting the adjacent shorted elements together, resulting in a continuous long strip. This geometrical simplification might seem surprising since we previously claimed that mutual coupling is really important for wideband performance. However, the affected elements are inactive and therefore mutual coupling had very little on bandwidth performance.

The 7  $\times$  7 dipole array used for measurements is depicted in Fig. 8(a). This array was also simulated including the CPW and

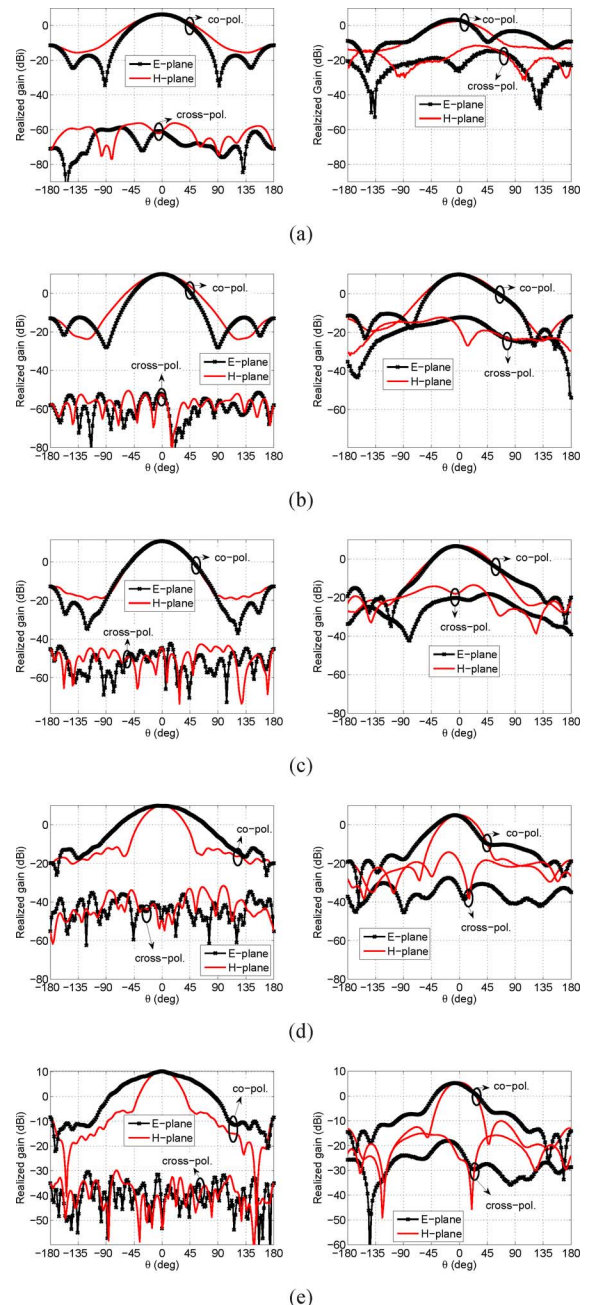


Fig. 11. (left) Simulated and (right) measured realized gain radiation patterns for the array in Fig. 8(a). Principal plane cuts are given at (a) 200 MHz, (b) 300 MHz, (c) 400 MHz, (d) 500 MHz, and (e) 600 MHz.

CPS lines, but not the baluns. In the simulations, feeding was done with 200- $\Omega$  ports placed at the bottom of the CPS feed lines for each active element. Also, for the corporate network VSWR calculation, an ideal 1:21 divider was assumed.

#### A. Broadside Scan

The array feed network for broadside scan is shown in Fig. 9. For the corporate feed a 1:3 power divider followed by three 1:8 power dividers were used to generate 24 equal power outputs. Three out of the 24 outputs were terminated in matched loads (see Fig. 9). From the available component data sheets, we calculated that the losses of the feed network (1:8 divider, 1:3 divider, divider terminations and balun) lowered the measured

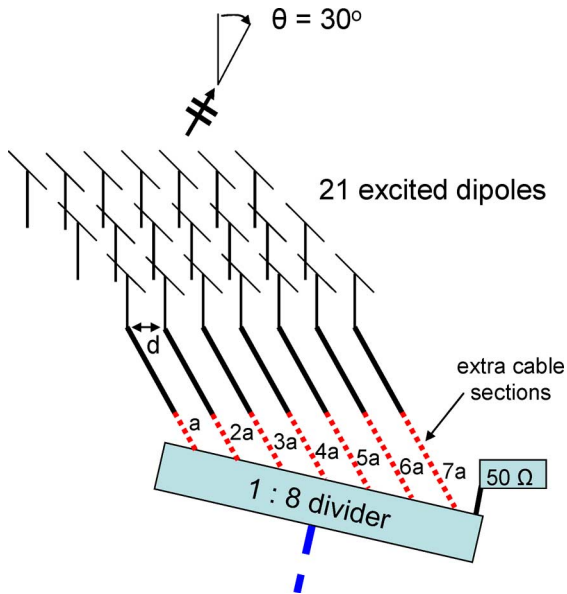


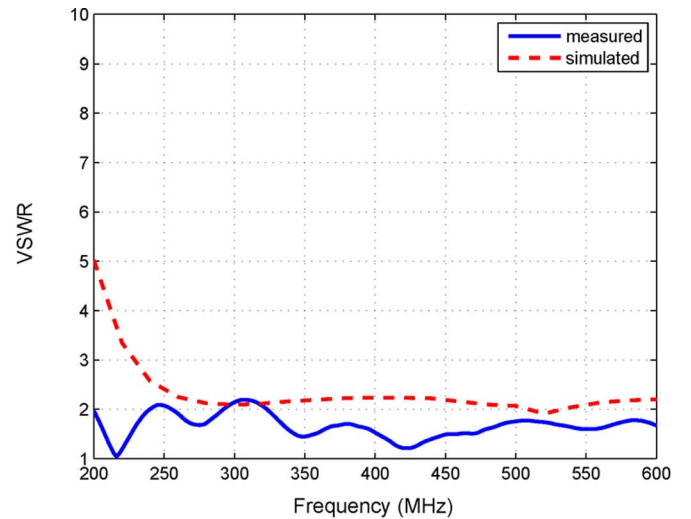
Fig. 12. Array feed network schematic for scanning at  $30^\circ$  in the H-plane (feeding of one column is shown only).

realized gain by about 2.8 dB. Measurements were carried out in the compact range of ElectroScience Laboratory, Ohio State University [see Fig. 8(b)]. We measured the array's corporate network VSWR, realized gain and radiation patterns on the E- and H-planes of the array. Fig. 10 depicts the measured and simulated corporate network VSWR.

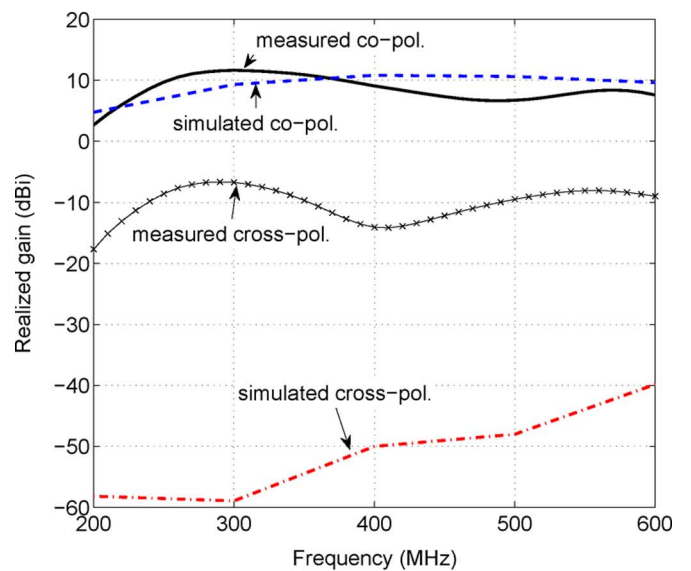
From Fig. 10(a) we observe that the measured VSWR is lower as compared to the simulated curves. This is due to losses in the actual feed network. Nevertheless, it indicates that the array does not suffer any unusual mismatches. Fig. 10(b) gives the measured and simulated co- and cross-polarized realized gain at broadside after accounting for the 2.8-dB feed network loss. As seen, the measured and simulated co-polarized realized gain curves are generally in agreement. Specifically, the array achieved a realized gain of  $>5$  dBi over the 200 MHz–600 MHz band.

Fig. 11 shows the measured and simulated radiation patterns for broadside scan. We observe that the measured radiation patterns exhibit narrower beamwidths than the simulated ones, particularly in the E-plane and at higher frequencies. This is most likely due to not including the feed network into the simulations. As mentioned above, the simulations were done using lumped ports at the bottom of the 200  $\Omega$  CPS lines. For our measurements (see Fig. 9), we employed 1:8 dividers along the H-plane, and 1:3 divider along the E-plane. Under ideal conditions, we would expect equal power distribution. However, because of inter-element coupling (stronger on the E-plane) there was impedance variation among the dividers' outputs, which led to nonuniform power distribution. Most likely, this is the reason for the discrepancy between the measured and simulated gain patterns. The fact that the differences are more pronounced in the E-plane provides further credence to the aforementioned explanation.

An other observation is that the measured cross-polarized gain is much higher than the simulated. This is likely



(a)



(b)

Fig. 13. Measured and simulated (a) VSWR and (b) realized gain for the array shown in Fig. 8(a) when fed for scanning at  $\theta = 30^\circ$  in the H-plane.

due to small misalignments of the array and the feeding antenna during measurements. To verify this, we calculated the simulated cross-polarized gain, while the array was slightly misaligned off broadside (i.e., at  $\theta = 1^\circ$ ,  $\phi = 2^\circ$ ). As seen, the cross-polarized gain does increase even when the array is misaligned  $1^\circ$  to  $2^\circ$  off broadside.

### B. Scanning at $30^\circ$ in the H-Plane

To scan at  $\theta_0 = 30^\circ$  in the H-plane we inserted an extra section of cable at the feed of each active column. This section was added after the 1:8 dividers, as shown in Fig. 12. The required length of this extra section was integer multiples of  $a = d/\sin(\theta_0)\sqrt{\epsilon_r} = d/2\sqrt{\epsilon_r}$ , where  $d = 8.71$  cm ( $2/7$ ) is the distance between dipoles and  $\epsilon_r = 2.1$  is the dielectric constant of the cable.

The measured corporate network VSWR is shown in Fig. 13(a). Again, this measurement is affected by the feed

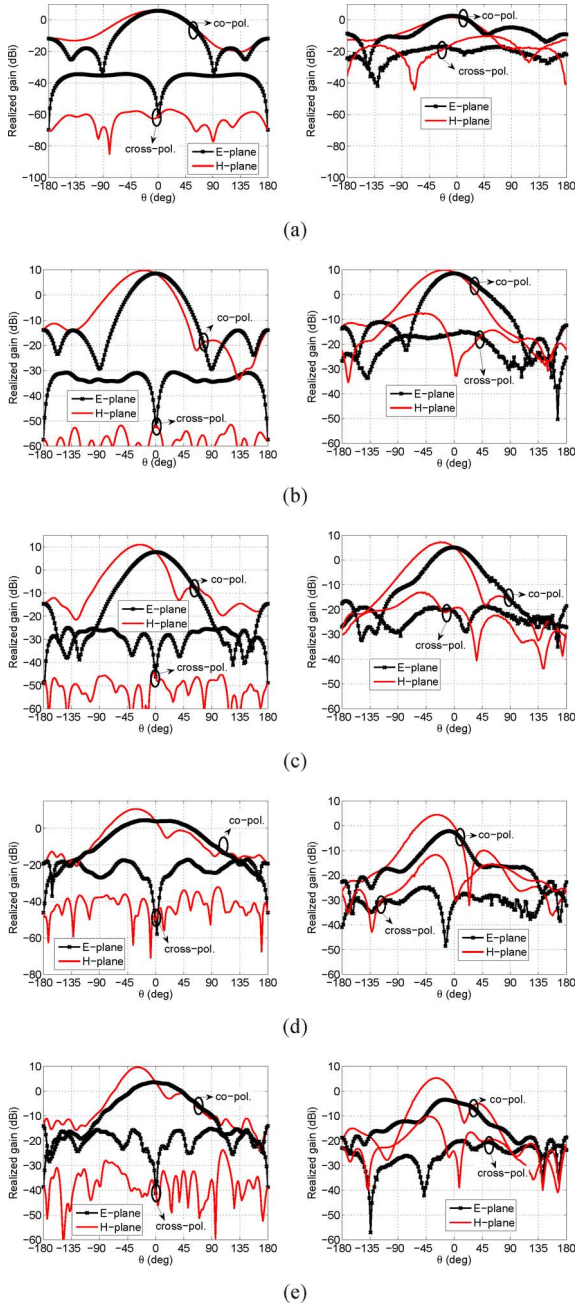


Fig. 14. (left) Simulated and (right) measured gain patterns for the array shown in Fig. 8(a) when fed for scanning at  $\theta = 30^\circ$  in the H-plane at (a) 200 MHz, (b) 300 MHz, (c) 400 MHz, (d) 500 MHz, and (e) 600 MHz.

network insertion loss. For comparison, the simulated corporate network VSWR is plotted in Fig. 13(a) assuming a lossless feed network. The measured and simulated gain at  $\theta = 30^\circ$  in the H-plane is shown in Fig. 13(b). As seen, the measured and simulated co-polarized gain curves are in agreement. Again, the measured cross-polarized gain was much higher than the simulated, likely due to array and feed misalignments. The measured and simulated realized gain patterns are depicted in Fig. 14. From these, we observe that instead of a fixed beam maximum at  $30^\circ$ , the patterns squint with frequency. This beam squint is attributed to the finite ground plane size as depicted in Fig. 15(a).

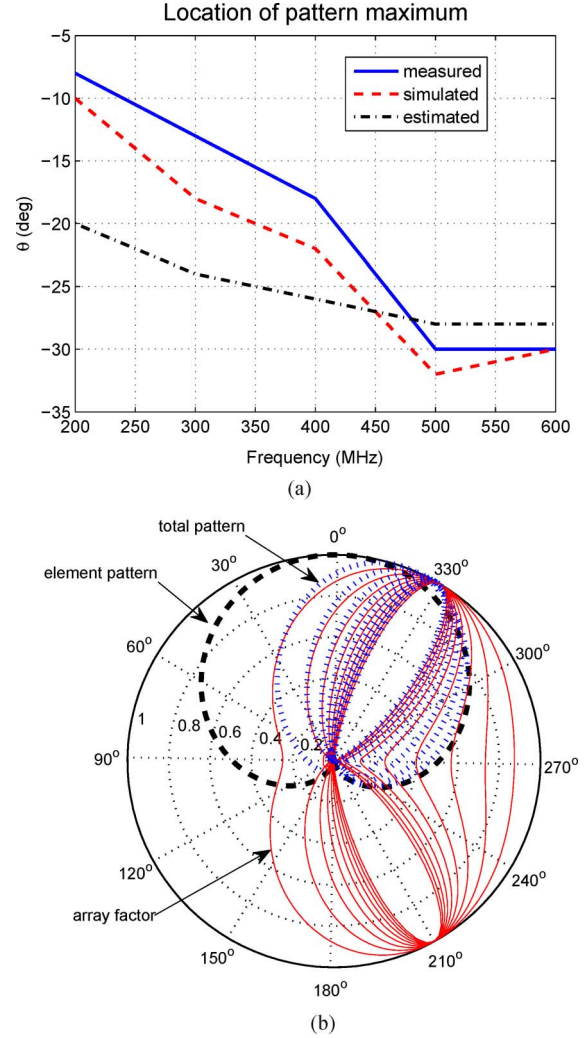


Fig. 15. (a) Measured, simulated, and estimated beam squint as a function of frequency. (b) Radiation pattern of a hypothetical seven-element linear dipole array with spacing 8.71 cm ( $2\lambda/7$ ), placed above a finite ground plane. Array is scanned to  $30^\circ$  in the H-plane. Beam squint with frequency can be observed in the total pattern [see also Fig. 15(a)].

To demonstrate that, we calculated the pattern of a hypothetical linear dipole array comprised of seven elements with spacing 8.71 cm ( $2\lambda/7$ ). To do that, we multiplied the element pattern with the array factor [26]. A typical H-plane pattern of a single dipole element over a finite ground plane is shown in Fig. 15(b). As seen, due to the finite ground plane size the element pattern tapers off as we move off of broadside ( $\theta = 0^\circ$ ) and eventually “folds” around it. The array factor for  $30^\circ$  scan in the H-plane was analytically calculated and is plotted in Fig. 15(b). Although the array factor maximum remains fixed at  $30^\circ$  for all frequencies, the array pattern squints because the element pattern is nonuniform, when radiating over a finite ground plane. Fig. 15(a) shows the theoretically estimated beam squint with frequency. Because of this beam squint, beam steering can not be performed using simple time delay at the feed. That is, the phase difference must be controlled more precisely.

#### IV. CONCLUSION

As would be expected, the bandwidth of tightly coupled phased arrays is degraded due to finite edge effects. A typical

strategy to alleviate edge effects [2] is to terminate the finite array elements at the periphery with matched loads/resistors. Although this approach improves array bandwidth, it reduces efficiency and realized gain.

In this paper, we demonstrated that instead of using resistive terminations, short-circuit terminations of the periphery elements provided for almost the same bandwidth performance, but also improved efficiency at lower frequencies by a maximum of 47%, implying a gain improvement of 2.75 dB. For demonstration, we designed and tested a  $7 \times 7$  overlapping dipole array  $60.96 \text{ cm} \times 60.96 \text{ cm}$  ( $2' \times 2'$ ) in size and 15.24 cm ( $6''$ ) thick. The array was placed on a  $121.92 \text{ cm} \times 121.92 \text{ cm}$  ( $4' \times 4'$ ) ground plane and was fed using a novel, printed, wideband feed, comprised of a CPW section interconnected to a short pair of CPS via a lumped balun. The array covered 200 MHz–600 MHz delivering a measured realized gain  $> 5$  dBi. The cross-pol. gain was also measured and found to be below  $-10$  dBi. A  $30^\circ$  H-plane scan was also measured. The realized gain at this scan angle was found to be  $> 3$  dBi over the whole band. In this process, we found that due to the finite ground plane (and the associated element pattern effects) the array beam squinted significantly from  $8^\circ$  at 200 MHz to  $30^\circ$  at 500 MHz.

#### ACKNOWLEDGMENT

The authors would like to thank the anonymous reviewers for their comments related to the measured radiation patterns. We truly believe that the review process resulted in an improved manuscript.

#### REFERENCES

- [1] B. Munk, *Finite Antenna Arrays and FSS*. Wiley, 2003.
- [2] M. Jones and J. Rawnick, "A new approach to broadband array design using tightly coupled elements," in *Proc. IEEE MILCOM '07*, Oct. 29–31, 2007, pp. 1–7.
- [3] J. Kasemodel and J. Volakis, "A planar dual linear-polarized antenna with integrated balun," *IEEE Antennas Wireless Propag. Lett.*, vol. 9, pp. 787–790, 2010.
- [4] J. Kasemodel, C.-C. Chen, and J. Volakis, "Low-cost, planar and wideband phased array with integrated balun and matching network for wideangle scanning," in *Proc. Antennas Propag. Soc. Int. Symp. (APSURSI)*, Jul. 2010, pp. 1–4.
- [5] S. Holland and M. Vouvakis, "A 7–21 GHz planar ultrawideband modular array," in *Proc. IEEE Antennas Propag. Soc. Int. Symp. (APSURSI)*, Jul. 2010, pp. 1–4.
- [6] I. Tzanidis, K. Sertel, and J. Volakis, "Characteristic excitation taper for ultra wideband tightly coupled antenna arrays," *IEEE Trans. Antennas Propag.*, vol. 60, no. 4, pp. 1777–1784, Apr. 2012.
- [7] A. Neto, D. Cavallo, G. Gerini, and G. Toso, "Scanning performances of wideband connected arrays in the presence of a backing reflector," *IEEE Trans. Antennas Propag.*, vol. 57, no. 10, pp. 3092–3102, Oct. 2009.
- [8] T. Vogler and W. Davis, "Analysis and modification of the infinite foursquare array," in *Proc. IEEE Antennas Propag. Soc. Int. Symp. (APSURSI)*, Jul. 2010, pp. 1–4.
- [9] J. Langley, P. Hall, and P. Newham, "Multi-octave phased array for circuit integration using balanced antipodal vivaldi antenna elements," in *Proc. Antennas Propag. Soc. Int. Symp. AP-S. Dig.*, Jun. 1995, vol. 1, pp. 178–181.
- [10] S. Livingston and J. Lee, "A wide band low profile dual-pol "Thumbtack" array," in *2010 IEEE Int. Symp. Phased Array Syst. Technol. (ARRAY)*, Oct. 2010, pp. 477–483.
- [11] J. Lee, S. Livingston, R. Koenig, D. Nagata, and L. Lai, "Long slot arrays - Part 2: Ultra wideband test results," in *Proc. IEEE Antennas Propag. Soc. Int. Symp.*, July 2005, vol. 1A, pp. 586–589.

- [12] R. Kindt and W. Pickles, "Ultrawideband all-metal flared-notch array radiator," *IEEE Trans. Antennas Propag.*, vol. 58, no. 11, pp. 3568–3575, Nov. 2010.
- [13] R. Guinvarc'h and R. Haupt, "Dual polarization interleaved spiral antenna phased array with an octave bandwidth," *IEEE Trans. Antennas Propag.*, vol. 58, no. 2, pp. 397–403, Feb. 2010.
- [14] H. Steyskal, J. Ramprecht, and H. Holter, "Spiral elements for broadband phased arrays," *IEEE Trans. Antennas Propag.*, vol. 53, no. 8, pp. 2558–2562, Aug. 2005.
- [15] I. Tzanidis, K. Sertel, and J. L. Volakis, "Interwoven spiral array (ISPA) with a 10:1 bandwidth on a ground plane," *IEEE Antennas Wireless Propag. Lett.*, vol. 10, pp. 115–118, 2011.
- [16] I. Tzanidis, K. Sertel, and J. Volakis, "Excitation and termination of finite tightly coupled antenna arrays based on structural characteristic modes," in *Proc. Antenna Applications Symp.*, Sep. 2011.
- [17] D. Cavallo, A. Neto, and G. Gerini, "Common-mode resonances in ultra wide band connected arrays of dipoles: Measurements from the demonstrator and exit strategy," in *Proc. Int. Conf. Electromagn. Adv. Applicat. ICEAA'09*, 2009, pp. 435–438.
- [18] D. Cavallo, A. Neto, and G. Gerini, "PCB slot based transformers to avoid common-mode resonances in connected arrays of dipoles," *IEEE Trans. Antennas Propag.*, vol. 58, no. 8, pp. 2767–2771, Aug. 2010.
- [19] J. Duncan and J. Minerva, "100:1 bandwidth balun transformer," *Proc. IRE*, vol. 48, no. 2, pp. 156–164, Feb. 1960.
- [20] S. March, "A wideband stripline hybrid ring (correspondence)," *IEEE Trans. Microw. Theory Tech.*, vol. MTT-16, no. 6, p. 361, Jun. 1968.
- [21] A. Vasylychenko, L. Wang, Z. Ma, W. De Raedt, and G. Vandenbosch, "A very compact CPW-to-CPS balun for UWB antenna feeding," in *Proc. IEEE 25th Conv. Elect. Electron. Eng.*, Dec. 2008, pp. 446–449.
- [22] Y.-H. Suh and K. Chang, "A wideband coplanar stripline to microstrip transition," *IEEE Microw. Wireless Compon. Lett.*, vol. 11, no. 1, pp. 28–29, Jan. 2001.
- [23] H. Phelan, "A wide-band parallel-connected balun," *IEEE Trans. Microw. Theory Tech.*, vol. MTT-18, no. 5, pp. 259–263, May 1970.
- [24] V. Trifunovic and B. Jokanovic, "Review of printed Marchand and double Y baluns: Characteristics and application," *IEEE Trans. Microw. Theory Tech.*, vol. 42, no. 8, pp. 1454–1462, Aug. 1994.
- [25] G. Guanella, "High-Frequency Matching Transformer," U.S. patent 2,470,307, May 17, 1949.
- [26] C. Balanis, *Antenna Theory: Analysis and Design*, 3rd ed. New York, NY, USA: Wiley-Interscience, 2005, ch. 12, pp. 653–738.



**Ioannis Tzanidis** (M'11) was born in 1983. He received the Diploma degree in electrical and computer engineering from Democritus University of Thrace, Xanthi, Greece, and the M.Sc. and Ph.D. degrees from The Ohio State University, Columbus, OH, USA, in 2010 and 2011, respectively.

In 2011, he was a Post-Doctoral Researcher at the ElectroScience Laboratory, The Ohio State University. In 2012, he joined the Samsung R&D center in Richardson, TX, USA. His research interests include wideband antennas, antenna miniaturization techniques, UWB arrays, array feeding techniques, and MIMO antennas.

Dr. Tzanidis received first place in the student paper competition of the Antennas and Propagation Symposium in 2010.

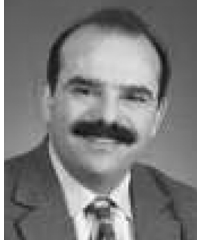


**Kubilay Sertel** (M'03–SM'07) received the Ph.D. degree from the Electrical Engineering and Computer Science Department, University of Michigan, Ann Arbor, MI, USA, in 2003.

He is currently an Assistant Professor at the Electrical and Computer Engineering Department, The Ohio State University. He was a Research Scientist at the ElectroScience Laboratory and an Adjunct Professor at the Electrical and Computer Engineering Department, The Ohio State University, from 2003 to 2012. His current research focuses

on the analysis and design of THz and mmW sensors, antennas arrays and spectroscopy systems for biomedical and nondestructive imaging, as well as ultra wideband low-profile antennas and phased arrays for cognitive sensing and opportunistic wireless networks, reconfigurable antennas, arrays and miniaturization techniques, novel RF materials, frequency selective surfaces/volumes and magneto-dielectric metamaterials, measurement and

characterization of anisotropic composites. His expertise also includes applied electromagnetic theory and computational electromagnetics, particularly, curvilinear fast multipole modeling of hybrid integral equation/finite element systems and efficient solution of large-scale, real-life problems on massively parallel supercomputing platforms.



**John L. Volakis** (S'77–M'82–SM'89–F'96) was born in Chios, Greece, on May 13, 1956. He received the B.E. degree (*summa cum laude*) from Youngstown State University, Youngstown, OH, USA, in 1978 and the M.Sc. and Ph.D. degrees from The Ohio State University, Columbus, OH, USA, in 1979 and 1982, respectively.

He started his career at Rockwell International (1982–1984), now Boeing. In 1984, he was appointed an Assistant Professor at the University of Michigan, Ann Arbor, MI, USA, becoming a Full Professor in 1994. He also served as the Director of the Radiation Laboratory from 1998 to 2000. Since January 2003, he has been the Roy and Lois Chope Chair Professor of Engineering at The Ohio State University, and also serves

as the Director of the ElectroScience Laboratory. Over the years, he carried out research in antennas, wireless communications and propagation, computational methods, electromagnetic compatibility and interference, design optimization, RF materials, multi-physics engineering, bioelectromagnetics, terahertz, and medical sensing. His publications include eight books (among them: *Approximate Boundary Conditions in Electromagnetics* (IEE, 1995); *Finite Element Methods for Electromagnetics* (IEEE, 1998); *4th edition Antenna Engineering Handbook* (McGraw-Hill, 200); *Small Antennas* (McGraw-Hill, 2010); and *Integral Equation Methods for Electromagnetics* (IET, 2011), over 320 journal papers, nearly 600 conference papers and 23 book chapters. He has graduated/mentored over 70 doctoral students/post-docs with 20 of them receiving best paper awards at conferences.

Prof. Volakis was 2004 President of the IEEE Antennas and Propagation Society, twice the general Chair of the IEEE Antennas and Propagation Symposium, IEEE APS Distinguished Lecturer, IEEE APS Fellows Committee Chair, IEEE-wide Fellows committee member and Associate Editor of several journals. He is listed by ISI among the top 250 most referenced authors (2004), and is a Fellow of ACES. Among his awards are: The University of Michigan College of Engineering Research Excellence award (1993), Scott award from The Ohio State University College of Engineering for Outstanding Academic Achievement (2011), and the IEEE AP Society C-T. Tai Teaching Excellence award (2011).